begell house, inc.
Journal Production
50 Cross Highway
Redding, CT 06896
Phone: 1-203-938-1300
Fax: 1-203-938-1304
Begell House Production Contact : journals@begellhouse.com

Dear Corresponding Author,

Effective April 2011 Begell House will no longer provide corresponding authors with a print copy of the issue in which their article appears. Corresponding authors will now receive a pdf file of the final version of their article that has been accepted for publication.

Please note that the pdf file provided is for your own personal use and is not to be posted on any websites or distributed in any manner (electronic or print). Please follow all guidelines provided in the copyright agreement that was signed and included with your original manuscript files.

Any questions or concerns pertaining to this matter should be addressed to journals@begellhouse.com

Thank you for your contribution to our journal and we look forward to working with you again in the future.

.

Sincerely,

Michelle Amoroso

Michelle Amoroso
Production Department

Journal of Porous Media, 15 (10): 937–953 (2012)

UTILIZATION OF MEMORY CONCEPT TO DEVELOP HEAT TRANSFER DIMENSIONLESS NUMBERS FOR POROUS MEDIA UNDERGOING THERMAL FLOODING WITH EQUAL ROCK AND FLUID TEMPERATURES

M. Enamul Hossain & Sidqi A. Abu-Khamsin*

Department of Petroleum Engineering, King Fahd University of Petroleum and Minerals, Dhahran 31261, Saudi Arabia

*Address all correspondence to M. Enamul Hossain E-mail: menamul@kfupm.edu.sa

Original Manuscript Submitted: 12/13/2010; Final Draft Received: 1/6/2012

Enhanced oil recovery (EOR) techniques are regaining interest as high oil prices have rendered such techniques economically attractive. Thermal EOR processes, which involve injection of heat into the reservoir, cause continuous alteration of the thermal characteristics of both reservoir rock and fluids that are seldom modeled in the heat and momentum transfer equations. In this study, the memory concept is employed to develop new dimensionless numbers that can characterize convective heat transfer between the rock and fluids in a continuous alteration phenomenon. The energy balance equation is employed to develop the heat transfer coefficient with the assumption that the rock achieves the fluid temperature instantaneously. The final form of the equation is written in terms of Peclet number and the three proposed dimensionless numbers. The results show that the proposed dimensionless numbers are sensitive to the absolute and effective thermal conductivities of the solid and fluids, average system heat capacity, and the hydraulic diffusivity of the fluid-saturated porous medium. One of the new numbers correlates with the Nusselt and Prandtl numbers, while the local Peclet number is found to be sensitive to memory. Since heat convection and conduction in porous media can now be explained through the proposed numbers with the memory concept, these numbers help characterize the rheological behavior of the rock–fluid system. This work will enhance understanding the effect of heat transfer on alteration of thermal conductivity during thermal recovery operations in a hydrocarbon reservoir.

KEY WORDS: *heat transfer coefficient, reservoir modeling, forced convection, Peclet number, temperature distribution, temperature profile, numerical simulation, reservoir management*

1. INTRODUCTION

A temperature difference within a physical system causes heat transfer to occur from the higher-temperature region to the lower-temperature region. This transport process continues until the system attains a uniform temperature. The heat flux, which is a function of temperature difference, depends on one or a combination of the various transport mechanisms, that is, conduction, radiation, or convection. While the first two mechanisms could be significant in any system, convective heat transfer is of utmost interest in porous media where fluid velocity is the major concern.

The temperature distribution in a hydrocarbon reservoir is an important issue due to its utilization in detecting water or gas influx or type of fluid entering into the wellbore. This information is necessary for better reservoir management, which is subject to reservoir rock–fluid rheologies. During thermal EOR operations, conversely, the highly complex characteristics of rock–fluid interac-

1091–028X/12/$35.00

NOMENCLATURE

A	cross-sectional area of rock perpendicular to the flow of flowing fluid, m^2	$L_{c-\mathrm{Ra}}$	characteristic length for Rayleigh number, m
		$L_{c-\mathrm{Re}}$	characteristic length for Reynolds number, m
c_f	total fluid compressibility of the system, 1/Pa	$L_{c-\mathrm{Sh}}$	characteristic length for Sherwood number, m
		$L_{c-\mathrm{We}}$	characteristic length for Weber number, m
c_s	formation rock compressibility of the system, 1/Pa	L^*	dimensionless length of the reservoir
		M	average system heat capacity, kJ/m^{3}K
c_t	total compressibility of the system, 1/Pa	N	rotational speed
c_{pf}	specific heat capacity of injected fluid, kJ/kg K	$(N_{\mathrm{Nu}L})_b$	$= h_c L_c/k_e$, local Nusselt number of bulk porous media saturated with fluid, dimensionless
c_{pg}	specific heat capacity of steam, kJ/kg K		
c_{po}	specific heat capacity of oil, kJ/kg K	$(N_{\mathrm{Nu}})_{x^*}$	$= h_c x^*/k_e$, local Nusselt number with respect to wellbore position toward the boundary of the reservoir, dimensionless
c_{ps}	specific heat capacity of solid rock matrix, kJ/kg K		
c_{pw}	specific heat capacity of water, kJ/kg K	$N_{\mathrm{Pe}L}$	$= L_c \rho_f c_{pf} u_m/k_e$, local Peclet number, dimensionless
D	diameter, m		
g	gravitational acceleration in x direction, m/s^2	N_{Pr}	$= \mu c_{pf}/k_e$, Prandtl number, dimensionless
h_c	convection heat transfer coefficient, kJ/hm^{2}K	$(N_{\mathrm{Pr}})_b$	$= v/\alpha_{Tb}$, bulk Prandtl number of fluid-saturated porous medium, dimensionless
k	absolute variable permeability, m^2	p	pressure of the system, Pa
k_e	effective thermal conductivity of fluid-saturated porous media, kJ/h m K	P_w	power, hp
		P_i	initial pressure of the system, Pa
k_f	absolute thermal conductivity of fluid within the porous rock matrix, kJ/h m K	a	reference pressure of the system, Pa
		q_i	$= Au$, initial volume production rate, m^3/s
k_g	thermal conductivity of gas, kJ/h m K	q_x	fluid mass flow rate per unit area in x direction, kg/m^{2}s
K_{mc}	mass transfer coefficient, m/s		
K_o	thermal conductivity of oil, kJ/h m K	q_*	dimensionless volume production rate
K_s	absolute thermal conductivity of solid rock matrix, kJ/h m K	q_{inj}	$= Au$, volume flow rate of injected hot water, m^3/s
K_w	thermal conductivity of water, kJ/h m K	q_{prod}	$= Au$, production volume flow rate of oil, m^3/s
L	distance between production and injection well along x direction, m	r_{pt}	pore-throat radius, microns
		S_g	gas saturation, volume fraction
L_c	characteristic length related to pore-throat diameter, m	S_o	oil saturation, volume fraction
L_{c-Bi}	$= V_{\mathrm{body}}/A_{\mathrm{surface}}$, characteristic length for Biot number, m	S_w	water saturation, volume fraction
		S_{wi}	initial water saturation, volume fraction
$L_{c-\mathrm{Bo}}$	characteristic length for Bond number, m	t	time, s
$L_{c-\mathrm{Fo}}$	characteristic length through which conduction occurs for Fourier number, m	t_c	characteristic time, s
		T	temperature, k
$L_{c-\mathrm{Gr}}$	characteristic length through which conduction occurs for Grashof number, m	T^*	dimensionless temperature
		T_f	temperature of injected fluid, K
$L_{c-\mathrm{Nu}}$	characteristic length for Nusselt number, m	T_f^*	dimensionless temperature of injected fluid
$L_{c-\mathrm{Pe}}$	characteristic length for Peclet number, m	T_i	initial reservoir temperature, K

NOMENCLATURE (Continued)

T_r	reference temperature of injected fluid, K
T_s	average temperature of solid rock matrix, K
T_s^*	dimensionless temperature of solid rock matrix
T_{st}	injected hot water temperature, K
t^*	dimensionless time
u_m	fluid velocity with memory in porous media in the direction of x axis, m/s
u^*	dimensionless velocity
V	fluid velocity for Reynolds number, m/s
V_L	characteristic velocity of liquid, m/s
x	flow dimension at any point along x direction, m
x^*	dimensionless distance

Greek Symbols

α	fractional order of differentiation, dimensionless
α_H	$= k/\varphi\mu c_t$, hydraulic diffusivity of the fluid-saturated porous medium, m^2/s
α_m	mass diffusivity, m^2/s
α_{Tb}	$= k_e/M$, bulk thermal diffusivity of fluid-saturated porous medium, m^2/s
α_{Ti}	thermal diffusivity at temperature T_s for Fourier number, m^2/s
β	$= 1/v\,(\partial v/\partial p)\,p$, volumetric thermal expansion coefficient, m^3/m^3K
ΔT	temperature difference, K
ν	$= \mu/\rho_f$, kinematic viscosity (ratio of absolute or dynamic viscosity to density), m^2/s
η	ratio of the pseudopermeability of the medium with memory to fluid viscosity, $m^3\ s^{1+\alpha}/kg$
μ	fluid dynamic viscosity, Pa s
μ_L	fluid dynamic viscosity for capillary number, Pa s
ξ	a dummy variable for time, i.e., real part in the plane of the integral, s
ξ^*	dimensionless dummy variable for time, i.e., real part in the plane of the integral
Γ	gamma function
ρ	fluid density, kg/m^3
$\Delta\rho$	$= \rho_w - \rho_o$, density difference of fluids (i.e., water and oil), kg/m^3
φ	porosity of the rock, volume fraction
ρ_f	density of fluid, kg/m^3
ρ_g	density of gas, kg/m^3
ρ_o	density of oil, kg/m^3
ρ_s	density of solid rock matrix, kg/m^3
ρ_w	density of water, kg/m^3
σ_{Bo}	surface tension of the interface or interfacial forces for Bond number, N/m
σ_{ca}	surface or interfacial tension between the two fluid phases for Capillary number, N/m
σ_{we}	surface tension for Weber number, N/m

Acronyms and Field Units

API	American petroleum institute
rb	reservoir barrels
stb	standard barrels
scf	standard cubic feet

tion play a vital role in heat transfer between the rock matrix and flowing hydrocarbons. Such heat transfer is the major factor governing the temperature profile within the reservoir. The previously mentioned complex phenomena can be explained by the concept of continuous time function, termed *memory*, to analyze the rheological behavior of rock and fluid properties when the rock is not in thermal equilibrium with the fluid(s) (Hossain and Abu-Khamsin, 2012).

The memory concept is of interest to researchers in different areas of science and engineering. Caputo and Plastino (2004) modified Darcy's constitutive equation with the introduction of the memory concept. They also modified the second constitutive equation of diffusion, which relates the density variations in the fluid to pressure, where they incorporated the memory formalisms. They computed the Green's function of pressure in the layer when a constant pressure is applied to the boundary for which they found closed-form formulae and attempted to capture the memory parameters experimentally. They concluded that the memory concept represents media in which the fluid flux decays more rapidly in time and delays the effect of the pressure at the boundary relative to the effects of the classic Darcy formula.

De Espiíndola et al. (2005) used the fractional derivative model (i.e., a measure of memory) to identify the dynamic properties of viscoelastic materials. They also presented numerical and experimental results where they claimed that no previous work had produced a technique for the identification of the fractional parameters of viscoelastic materials directly from an experiment. To validate the procedure, a comparison of the measured and regenerated transmissibility was made. Storage modulus and loss factors were computed using the minimizing parameters of a particular cost function. These functions were then plotted in terms of frequency and temperature.

Cloot and Botha (2006) used the generalized classical Darcy law, where they used a noninteger order derivative of the piezometric head for groundwater flow. Numerical solutions of their equation for various fractional orders of the derivatives were compared with experimental data to see the behavior of fractional derivatives of modified Darcy's law.

For porous media application, Iaffaldano et al. (2006) conducted an experiment to capture the permeability changes with time for a sand layer. They also provided a memory model for diffusion of fluids in porous media, which matched well with the flux rate observed in experiments. They concluded that the flux rate variations observed during the experiments were compatible with the compaction of sand. This variation was due to the amount of fluid that went through the grains locally. As a result, there was a reduction of porosity.

Zavala-Sanchez et al. (2009) investigated solute transport in a vertically bounded stratified random medium. They studied the effective mixing and spreading dynamics at preasymptotic times in terms of effective average transport coefficients, which had been defined on the basis of local moments, that is, moments of the transport Green function. They quantified the disorder-induced mixing and spreading by a constant Taylor dispersion coefficient. They observed the impact of the position of the initial plume and the initial plume size on the preasymptotic effective spreading and mixing dynamics for single realizations. They showed that the system "remembers" its initial state, which was defined as memory effects for the effective transport coefficients. This memory effect disappeared after the solute had sampled the full vertical extent of the medium.

Recently, Di Giuseppe et al. (2010) modified the constitutive equations by introducing a memory formalism operating on both the pressure gradient–flux and the pressure–density variations where fractional order derivatives were used to represent the memory formalism. They conducted sets of laboratory experiments in uniformly packed columns for both homogeneous and heterogeneous media where a constant pressure was applied on the lower boundary. They concluded that the memory largely influenced the experiments; they showed how mechanical compaction can decrease permeability and, consequently, flux, through data and theory. Moreover, memory can be affected by the tank height, the particle size distribution, the stability of the initial particle distribution, and so on.

In EOR processes, alteration of rock–fluid properties during thermal recovery is well established in the literature (Hossain et al., 2007, 2008a, 2008b, 2009a; Hossain and Islam, 2009). This alteration occurs because when a fluid flows through a porous medium, the permeability of the matrix may vary locally with time (Iaffaldano et al., 2006; Cloot and Botha, 2006) for several reasons: chemical dissolution of the medium, swelling and flocculation, pore plugging and precipitation reactions, transport of particles obstructing the pores, mechanical compaction, and grain crumbling due to high pressure (Di Giuseppe et al., 2010). All these phenomena, in conjunction with possible chemical reactions between the fluid and the medium, create continuous local changes of both porosity and permeability, resulting in memory; that is, at a given instant in time, the advection process is affected by the history of pressure and flux (Iaffaldano et al., 2006; Di Giuseppe et al., 2010). Most importantly, the alteration of rock and fluid properties guides the temperature profile within the reservoir formation. Published literature shows that the fluid velocity (Yoshioka et al., 2005a, 2005b) and time have strong effects on the temperature profile (Hossain, 2008; Hossain et al., 2008a, 2008b). Therefore it is important to investigate the effects of memory in terms of different heat transfer dimensionless numbers based on the rheology of the rock–fluid system.

Convection and conduction heat transfer depends on the fluid temperature, which is related to surroundings' temperature, surroundings' conductivity (i.e., limestone, seawater, and air), insulation, inner-film conductivity, and residence time. The available models are unable to handle the alteration of rock and fluid properties with time during thermal operations (Marx and Langenheim, 1959; Willman et al., 1961; Spillette, 1965; Chan and Banerjee, 1981; Kaviany, 2002). Recent investigations show that due to memory and temperature variation in the formation, the porosity, permeability, and rheology of the reservoir may change as a result of continuous heat transfer within the fluid and rock matrix (Hossain et al., 2007, 2009a; Hossain, 2008). However, previous works did not consider the thermal effects in terms of Peclet number and

other heat transfer coefficients when the rock and fluid temperatures are considered equal ($T_s = T_f$). In addition, the continuous alteration of fluid and pore space properties may be greatly influenced by the fluid memory, especially in geothermal reservoirs (Hossain et al., 2007, 2009a; Hossain, 2008). Hossain et al. (2009a) showed how stress–strain relationships can be presented and characterized through the memory concept. They did not use this concept for thermal recovery processes.

Therefore the present paper shows the effects of including the memory function in the fluid flow behavior during hot water injection into a hydrocarbon reservoir. As discussed earlier, fluid velocity and time have strong effects on the temperature profile. Thus it is very important to investigate the effects of fluid memory as well as the rheology of the rock–fluid system based on heat transfer coefficients.

In this study, model equations developed by Hossain and coauthors (Hossain et al., 2011; Hossain and Abu-Khamsin, 2012) are employed to investigate the major role of alteration of various rock and fluid properties during thermal operations in terms of Peclet number and three proposed dimensionless numbers associated with heat transfer in porous media. While those studies were conducted for unequal rock and fluid temperatures, the present study assumes that the rock attains the fluid's temperature instantaneously, that is, that the rock and fluid temperatures are equal throughout the system. The main objective of this study is to characterize different heat transfer dimensionless numbers that are sensitive to the time dimension. The model equation describes how the fluid and rock properties are dependent on the continuous time function. Thus the equation affords investigation of the dependence of different heat transfer coefficients—in terms of dimensionless numbers—on the system's parameters and properties. To solve the model equation for different dimensionless numbers, MATLAB programming was used. This analysis will provide a better understanding of heat transfer phenomena during thermal operations in porous media.

2. MATHEMATICAL FORMULATION

The model considers a porous medium of uniform cross-sectional area and that is homogeneous along the x axis. Normal practice assumes fluid flow in porous media to be governed by Darcy's law. In this study, however, the modified Darcy's law is employed to introduce the notion of fluid memory (Caputo, 1999, 2000; Hossain et al., 2008c; Hossain and Islam, 2009). Before commencement of hot fluid injection, both pressure and temperature are assumed to be uniform throughout the reservoir. Since the medium is homogeneous, the pressure along the x direction may be considered to vary initially according to the Darcy diffusivity equation. It is also considered that the thermal conductivities of both fluid and solid rock matrices are not functions of temperature and are constant throughout the reservoir.

To develop the new dimensionless numbers, the temperature distribution pattern is developed based on the energy balance equation (Hossain et al., 2011). In this regard, the equation is considered as the governing equation for both rock and fluid separately. The inclusion of time-dependent rock and fluid properties is of great significance to petroleum engineers because prediction of production performance and management is highly uncertain. Therefore consideration of time-dependent phenomena is necessary for a well-managed petroleum project. Inclusion of the memory concept is made using the modified Darcy's law as the flow rate equation, which may be written for a 1-D system as (Hossain et al., 2007, 2008c, 2009b)

$$u_m = -\frac{\eta}{\Gamma(1-\alpha)} \int_0^t (t-\xi)^{-\alpha} \left[\frac{\partial^2 p}{\partial \xi \partial x}\right] \partial \xi \quad (1)$$

Hossain et al. (2008c) defined the composite variable, η, which is a function of permeability and viscosity, for any type of reservoir as

$$\eta = \frac{k}{\mu_{ab}} (t)^{\alpha} \quad (2a)$$

For example, Eq. (2a) can be expressed for sandstone as (Hossain et al., 2008c)

$$\eta = \frac{\left[3.0\,(p/6894.76)^{-0.31}\right] \times 10^{-12}}{\mu_{ob} e^{8.422\times10^{-5}(p-p_b)}} (t)^{\alpha} \quad (2b)$$

where

$$\mu_{ob} = 6.59927 \times 10^5 R_s^{-0.597627} T^{-0.941624} \gamma_g^{-0.555208} \times \mathrm{API}^{-1.487449}$$

$$p_b = -620.592 + 6.23087 \frac{R_s \gamma_o}{\gamma_g B_o^{1.38559}} + 2.89868T$$

$$B_o = B_{ob} e^{-C_o(p-p_b)}$$

$$B_{ob} = 1.122018 + 1.410 \times 10^{-6} \frac{R_s T}{\gamma_o^2}$$

$$C_o = \frac{\begin{pmatrix} -70603.2 + 98.404R_s + 378.266T \\ -6102.03\gamma_g + 755.345API \end{pmatrix}}{p + 3755.53}$$

Equation (2b) is based on field units, which are oil formation volume factor (B_o), rb/stb; oil compressibility (C_o), psi^{-1}; oil formation volume factor at the bubble point (B_{ob}), rb/stb; oil viscosity at the bubble point (μ_{ob}), cp; oil viscosity above the bubble point (μ_{ab}), cp; solution gas oil ratio (R_s), $\mathrm{scf/stb}$; crude oil temperature (T), °F; gas specific gravity (γ_g),$\mathrm{lb_m/ft^3}$; oil specific gravity (γ_o),$\mathrm{lb_m/ft^3}$; and oil API gravity (API), °API.

If the temperatures of the fluid and rock matrix are the same, the energy balance equations can be combined into a single equation [Eq. (3)] as used by several authors (Kaviany, 1995; Lee and Vafai, 1999; Alazmi and Vafai, 2000; Nield and Bejan, 2006). A detailed derivation of Eq. (3) is presented in the appendix and appears as Eq. (A14):

$$M\frac{\partial T}{\partial t} + \rho_f c_{pf} u_m \frac{\partial T}{\partial x} - k_e \frac{\partial^2 T}{\partial x^2} - = 0 \qquad (3)$$

Equation (3) can be transformed into dimensionless form using the following nondimensional parameters:

$$T^* = \frac{T}{T_i},\ T_s^* = \frac{T_s}{T_i},\ T_f^* = \frac{T_f}{T_i},\ x^* = \frac{x}{L},$$
$$p^* = \frac{p}{p_i},\ q^* = \frac{q}{q_i},\ t^* = \frac{kt}{\phi\mu c_t L^2},\ \xi^* = \frac{k\xi}{\phi\mu c_t L^2}$$

Using these parameters, the final form of Eq. (3) is obtained as [Appendix, Eq. (A18)]

$$\frac{\partial^2 T^*}{\partial x^{*2}} - N_{HA4}\frac{\partial T^*}{\partial t^*} - N_{\mathrm{Pe}L}\frac{L}{L_c}\frac{\partial T^*}{\partial x^*} = 0 \qquad (4a)$$

Now introducing a new dimensionless ratio, $N_{HA3} = (k_s + k_f)/k_e$, Eq. (4a) can be written as

$$\frac{1}{N_{HA3}}\frac{\partial^2 T^*}{\partial x^{*2}} - \frac{N_{\mathrm{Pe}L}}{N_{HA3}}\frac{L}{L_c}\frac{\partial T^*}{\partial x^*} - \frac{N_{HA4}}{N_{HA3}}\frac{\partial T^*}{\partial t^*} = 0 \qquad (4b)$$

where

$$N_{HA3} = \frac{k_s + k_f}{k_e} \qquad (5)$$

$$N_{HA4} = \frac{M\alpha_H}{k_e} \qquad (6)$$

$$k_e = \phi k_f + (1 - \phi)\, k_s \qquad (7)$$

Equations (4a) and (4b) give the dimensionless temperature profile and heat transfer along the formation length when the rock and fluid temperatures are considered equal. This model has been developed using the memory concept. Therefore, during the numerical computation, u_m is used to the find the impact of the memory function, while temperature distribution is governed by Eq. (4a) or (4b). This partial differential equation is solved to find the effects of different rock–fluid parameters in terms of Peclet number and three proposed numbers. Computations on Eq. (4b) are carried out for different rock–fluid parameters, where the initial and boundary conditions are defined as $T_f\,(x,0) = T_s\,(x,0) = T_i$ in terms of dimensionless form $T_f^*\,(x,0) = T_s^*\,(x,0) = 1$; $T_f\,(0,t) = T_s\,(0,t) = T_{st}$ in terms of dimensionless form $T_f^*\,(0,t) = T_s^*\,(0,t) = T_{st}/T_i$; and $T_f\,(L,t) = T_s\,(L,t) = T_i$ in terms of dimensionless form $T_f^*\,(L,t) = T_s^*\,(L,t) = 1$.

3. SIGNIFICANCE OF THE PROPOSED DIMENSIONLESS NUMBER

There are at least 15 dimensionless numbers associated with fluid dynamics and heat and mass transfer. Those numbers are summarized in Table 1. The proposed number 3 [Eq. (5)] can be defined as the ratio of the total absolute thermal conductivities of the fluid and rock to the effective thermal conductivity of the fluid-saturated porous medium, that is,

$$N_{HA3} = \frac{k_s + k_f}{k_e} = \frac{\begin{array}{c}\text{Total absolute}\\ \text{thermal conductivity of}\\ \text{fluid and rock matrix}\end{array}}{\begin{array}{c}\text{Effective thermal}\\ \text{conductivity of fluid-}\\ \text{saturated porous medium}\end{array}} \qquad (8)$$

Introducing a new dimensionless number, (N_{AH}), defined as

$$N_{AH} = \frac{\nu}{\alpha_H} \qquad (9)$$

the proposed number is the ratio of the fluid's kinematic viscosity to the system's (i.e., the fluid-saturated porous medium) hydraulic diffusivity. It is similar to the Schmidt number (Table 1) but replaces the fluid's mass diffusivity with the system's hydraulic diffusivity, which incorporates the effect of the rock matrix. Kinematic viscosity, also called the *momentum diffusivity*, is the ability of a fluid to transport momentum by molecular "diffusion." Since hydraulic diffusivity is the ratio of the system's fluid transmissivity to the system's fluid storativity, N_{AH} becomes a measure of the system's diffusive to convective momentum transport capability, as influenced by its compressibility. For sandstone of 0.2 porosity and

TABLE 1: Proposed new dimensionless number and different other dimensionless numbers used in heat transfer and fluid dynamics (Hossain and Abu-Khamsin, 2012)

Name	Symbol	Definition	Comments
Biot	N_{Bi}	$N_{\mathrm{Bi}} = (h_c L_{c-\mathrm{Bi}})/k_s$	Ratio of conductive to convective heat transfer resistance
Bond	N_{Bo}	$N_{\mathrm{Bo}} = (\Delta\rho g L^2_{c-\mathrm{Bo}})/\sigma_{\mathrm{Bo}}$	Ratio of body forces (often gravitational) to surface tension forces, i.e., interfacial forces
Capillary	N_{ca}	$N_{ca} = (\mu_{\mathrm{L}} v_{\mathrm{L}})/\sigma_{ca}$	Ratio of viscous forces to interfacial forces or surface tension
Fourier	N_{Fo}	$N_{\mathrm{Fo}} = (\alpha_{\mathrm{T_s}} t_C)/L^2_{c-\mathrm{Fo}}$	Ratio of the heat conduction rate to the rate of thermal energy storage; also expressed as a ratio of current time to reach steady state
Grashof	N_{Gr}	$N_{\mathrm{Gr}} = (g\beta\Delta T L^3_{c-\mathrm{Gr}})/\nu^2$	Ratio of the buoyancy to viscous force acting on a fluid; also a ratio of natural convection buoyancy force to viscous force
Proposed number 1	N_{HA1}	$N_{HA1} = (k\rho_f)/(\mu^2 c_t)$ $= \{N_{pr}\}_e/\{N_{pr}\}_f$	Ratio of the Prandtl number of the fluid-saturated porous medium to the Prandtl number of the fluid
Proposed number 2	N_{HA2}	$N_{HA2} = (1-\phi)/\phi$ $\times(\rho_s c_{ps})/(\rho_f c_{pf})$	Ratio of the heat transfer of solid matrix to the heat transfer of reservoir fluid
Proposed number 3	N_{HA3}	$N_{HA3} = (k_s + k_f)/k_e$	Ratio of total absolute thermal conductivity of fluid and rock to the effective thermal conductivity of the fluid-saturated porous medium; a new dimensionless number for fluid-saturated rock
Proposed number 4	N_{HA4}	$N_{HA4} = \alpha_H/\alpha_{Tb}$ $= \{N_{pr}\}_{\mathrm{b}}/N_{AH}$	Ratio of the bulk Prandtl number of the fluid-saturated porous medium to the proposed number; a new dimensionless number for fluid-saturated rock
Proposed number 5	N_{AH}	$N_{AH} = \nu/\alpha_H$	Ratio of the fluid's momentum diffusivity to the system's (fluid-saturated porous medium) hydraulic diffusivity; a new dimensionless number for fluid-saturated rock
Nusselt	N_{Nu}	$N_{\mathrm{Nu}} = (h_c L_{c-\mathrm{Nu}})/k_e$	Ratio of convective to conductive heat transfer across (i.e., normal to) the boundary
Peclet	N_{pe}	$N_{pe} = (\rho_f c_{pf} u_x L_{c-\mathrm{Pe}})/k_e$ $= (u_x L_{c-\mathrm{Pe}})/\alpha_{T_f}$	Ratio of convective to diffusive heat/mass transport in a fluid
Power	N_{po}	$N_{po} = P_w/(\rho N^3 D^5)$	Also known as Newton number and a ratio of resistance force to the inertia force
Prandtl	N_{pr}	$N_{pr} = \nu/\alpha_{T_f} = (\mu c_{pf})/k_f$	Ratio of momentum diffusivity (kinematic viscosity) and thermal diffusivity, or ratio of viscous diffusion rate to thermal diffusion rate
Rayleigh	N_{Ra}	$N_{\mathrm{Ra}} = N_{\mathrm{Gr}} N_{\mathrm{Pr}}$ $= (g\beta\Delta T L^3_{c-\mathrm{Ra}})/(\nu\alpha_{T_f})$	Ratio of buoyancy forces and the product of thermal and momentum diffusivities; ratio of natural convective to diffusive heat/mass transport; determines the transition to turbulence

TABLE 1 (Continued)

Name	Symbol	Definition	Comments
Reynolds	N_{Re}	$N_{\mathrm{Re}} = (\rho V L_{c-\mathrm{Re}})/\mu$	Ratio of inertial forces $\left(\rho V^2 L^2\right)$ to viscous forces $(\mu V L)$; ratio of convective to viscous momentum transport
Schmidt	N_{Sc}	$N_{\mathrm{Sc}} = \nu/\alpha_m = \mu/(\rho\alpha_m)$	Ratio of momentum diffusivity (viscosity) and mass diffusivity and used to characterize fluid flows in which there are simultaneous momentum and mass diffusion convection processes
Sherwood	N_{Sh}	$N_{\mathrm{Sh}} = (K_{mc} L_{c-\mathrm{Sh}})/\alpha_m$	Ratio of convective to diffusive mass transport; also called the mass transfer Nusselt number and used in mass transfer operations
Weber	N_{We}	$N_{\mathrm{We}} = (\rho V^2 L_{c-\mathrm{We}})/\sigma_{\mathrm{We}}$	A measure of the relative importance of the fluid's inertia compared to its surface tension and related to surface behavior for a two- phase system

0.1×10^{-12} m^2 absolute permeability, N_{AH} would be about 2.0×10^{-6} if the rock is saturated with air at ambient conditions. For the same sandstone, if saturated with freshwater, N_{AH} would be about 1.4×10^{-5}, which is 7 times larger due to water's larger ν (kinematic viscosity) and the water-saturated system's smaller α_H.

Manipulating Eq. (6) yields

$$N_{HA4} = \frac{M\alpha_H}{k_e} = \frac{\alpha_H}{\alpha_{Tb}} = \frac{\nu}{\nu}\frac{\alpha_H}{\alpha_{Tb}} = \frac{\nu/\alpha_H}{\nu/\alpha_{Tb}} = \frac{(N_{\mathrm{Pr}})_b}{N_{AH}} \tag{10}$$

The proposed number 4 (N_{HA4}) is the ratio of the hydraulic diffusivity to the thermal diffusivity—both of the fluid-saturated porous media—within the system volume. In essence, it is the ratio of the convective ability of the fluid-saturated porous medium to its conductive ability. Equation (10) also shows that (N_{HA4}) can be looked at as the ratio of the bulk Prandtl number of the fluid-saturated porous medium to its proposed number 5 (N_{AH}). Therefore N_{HA4} expresses the influence of the rock matrix on the thermal and flow characteristics of the fluid within the porous medium. The three dimensionless numbers proposed in this article are also listed in Table 1. Two dimensionless numbers proposed previously (Hossain and Abu-Khamsin, 2012) are listed in this table as well.

Again, Eq. (6) can be manipulated into

$$N_{HA4} = \frac{M\alpha_H}{k_e} = \frac{M\alpha_H}{h_c L_c}\frac{h_c L_c}{k_e} = \frac{M\alpha_H}{h_c L_c}(N_{\mathrm{Nu}L})_b = \frac{(N_{\mathrm{Nu}L})_b}{(h_c L_c)/(M\alpha_H)} \tag{11}$$

In Eq. (11), the proposed number 4 (N_{HA4}) is the ratio of the local bulk Nusselt number—that is, for the whole fluid-saturated porous medium—to the system's heat transfer mechanism, that is, both conduction and convection. Therefore N_{HA4} explains the correlation and influence of the system's heat transfer mechanism on the Nusselt number, where continuous alteration of rock–fluid properties can be linked up with time and Nusselt number during any thermal recovery process.

4. RESULTS AND DISCUSSION

Computations are carried out for a reservoir 3000 m long, where hot water is injected at a constant rate of 17.5 m^3 of equivalent water volume per day. All assumed rock and fluid parameters are listed in Table 2. The time and distance steps are set at $\Delta x^* = 0.0167$ and $\Delta t^* = 0.00001$. Temperature variation is obtained for the case where the fluid and rock temperatures are equal. In Eqs. (4a) and (4b), the local Peclet number can be defined as $(N_{\mathrm{Pe}})_L = L_c \rho_f c_{pf} u_m / k_e$, where L_c represents a characteristic length such as the mean pore throat diameter of the porous medium. During the computation, L_c is calculated by Winlad's (Kolodzie, 1980) correlation, $L_c = 2\pi r_{pt}$ and $\log r_{pt} = 0.732 + 0.588 \log k - 0.864 \log \phi$, where k is in mD and r_{pt} is in microns. Kolodzie (1980) and Pittman (1992) proposed the preceding correlation as the best permeability estimator for sandstones. They and others (Rezaee et al., 2006) indicated that the best results are obtained from a mercury injection capillary pressure test at 35% mercury saturation. Other correlations for carbonate rocks are also proposed in the same literature. During the computation of $(N_{\mathrm{Nu}L})_b$, the same procedure is

TABLE 2: Fluid and rock property values for numerical computation

Fluid and rock properties	Fluid and rock properties
c_{pg}= 29.7263 [KJ/Kg - K]	S_g = 20% [vol/vol]
c_{po} = 2.0934 [KJ/Kg - K]	S_o = 60% [vol/vol]
c_{ps} = 0.8792 [KJ/Kg - K]	S_w = 20% [vol/vol]
c_{pw} = 4.1868 [KJ/Kg - K]	T_{st} = 550 K
h_c = 280.87 [KJ/h - m^2 - K]	T_i = 300 K
k_g = 0.0143 [KJ/h - m - K]	$\rho_g = 16.7121$ [Kg/m^3]
k_o = 1.3962 [KJ/h - m - K]	$\rho_o = 800.923$ [Kg/m^3]
k_s = 9.346 [KJ/h - m - K]	$\rho_s = 2675.08$ [Kg/m^3]
k_w = 3.7758 [KJ/h - m - K]	$\rho_w = 1000.0$ [Kg/m^3]
$k_i = 10^{-15}$ [m^2]	$\phi = 25\%$ [m^3/m^3]
p_i = 48263299.0 [pa]	$\mu_f = 10$ pa.s [Ns/m^2]
$c_f = 1.2473 \times 10^{-9}$ [1/pa]	$q_i = 17.5$ m^3/d [110 bbl/day]
$c_s = 5.8015 \times 10^{-10}$ [1/pa]	$A = 300$ m $\times$ 20 m = 6000 m^2

used to calculate the L_c for local N_{HA4} and $(N_{\mathrm{Nu}}L)_b$. Moreover, as Nusselt number, N_{Nu}, refers to the ratio of total to conductive heat transfer, the local Nusselt number with respect to wellbore position and reservoir boundary can be defined as $(N_{\mathrm{Nu}})_{x^*} = [\partial T^*/\partial y^*]_{x^*=0,1}$, while it can also be calculated using $(N_{\mathrm{Nu}})_{x^*} = h_c x^*/k_e$.

Figures 1(a)–1(c) show the variation of the proposed number 3 (N_{HA3}) with the solid's (k_s), the fluid's (k_f), and the total ($k_s + k_f$) absolute thermal conductivity for various effective thermal conductivities (k_e). N_{HA3} increases linearly with the increase in k_s for a particular k_e value and decreases with the increase in k_e [Figs. 1(a) and 1(b)]. The same trend is seen in Fig. 1(c), however, the rate of increase of N_{HA3} is lower than in Figs. 1(a) and 1(b). This indicates that the solid's thermal conductivity is more dominant on N_{HA3} compared with the fluid's conductivity. Therefore conduction heat transfer has a greater influence on N_{HA3}.

Figure 2 depicts the variation of the proposed number 3 (N_{HA3}) with effective thermal conductivity (k_e) for various total absolute thermal conductivities ($k_s + k_f$). N_{HA3} decreases nonlinearly with the increase in k_e for a particular ($k_s + k_f$) value and increases with increase in ($k_s + k_f$). Again, this implies the great influence of conduction heat transfer on N_{HA3}.

Figures 3(a) and 3(b) show the variation of the proposed number 4 (N_{HA4}) with effective thermal conductivity (k_e) for different average system heat capacities (M) and for different hydraulic diffusivities of the fluid-saturated porous medium (α_H). N_{HA4} decreases nonlinearly with increase in k_e for a particular M, and both slope and nonlinearity of the curve increases for higher M [Fig. 3(a)]. N_{HA4} also increases with increase in M. Therefore the system's heat capacity has an influence on N_{HA4}, which means both conduction and convection heat transfer play a significant role on N_{HA4}. The same nonlinear trend is seen in Fig. 3(b). However, for low α_H, N_{HA4} does not change significantly with increase in k_e. As α_H increases, the degree of nonlinearity and the slope increase steadily for N_{HA4} versus k_e plots.

Figures 4(a) and 4(b) depict variation of the proposed number 4 (N_{HA4}) with different average system heat capacities (M) for different effective thermal conductivities (k_e) and different hydraulic diffusivities of the fluid-saturated porous medium α_H, N_{HA4} increases nonlinearly with increase in M for a particular k_e value, and N_{HA4} decreases with increase in k_e value for a particular M value [Fig. 4(a)]. A slightly sloping linear trend is shown for N_{HA4} versus M plots in Fig. 4(b). However, with increase in hydraulic diffusivity, N_{HA4} increases for a particular M value, which is more sensitive for larger α_H.

Figures 5(a) and 5(b) depict variation of the proposed number 4 (N_{HA4}) with hydraulic diffusivity α_H for different average system heat capacities (M) and for different effective thermal conductivities (k_e)—all for the fluid-saturated porous medium. N_{HA4}increases linearly with increase in α_H for a particular M value and the slope of the trend increases with increase in M value [Fig. 5(a)]. Conversely, N_{HA4} decreases with increase in k_e value

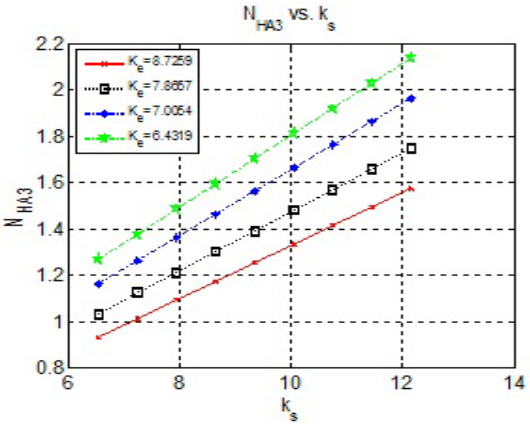

(a)

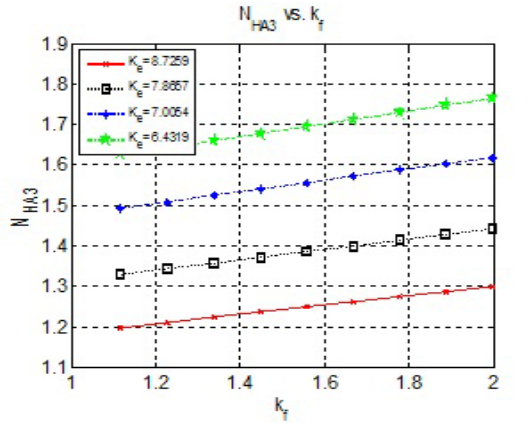

(b)

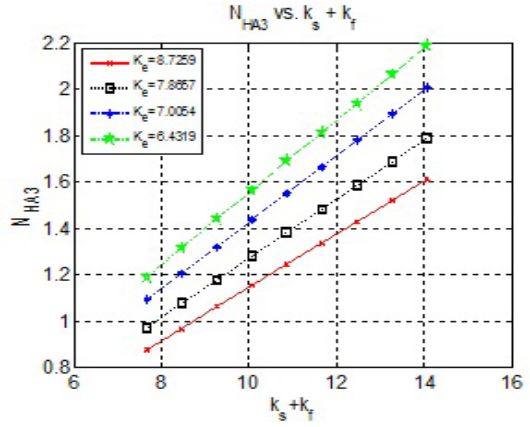

(c)

FIG. 1: Variation of the proposed number 3 (N_{HA3}) with absolute thermal conductivity of solid (k_s) at a given $k_f = 1.5957$ KJ/hmK, fluid (k_f) at a given $k_s = 9.346$ KJ/hmK, and total solid and fluid $(k_s + k_f)$ for different effective thermal conductivites (k_e)

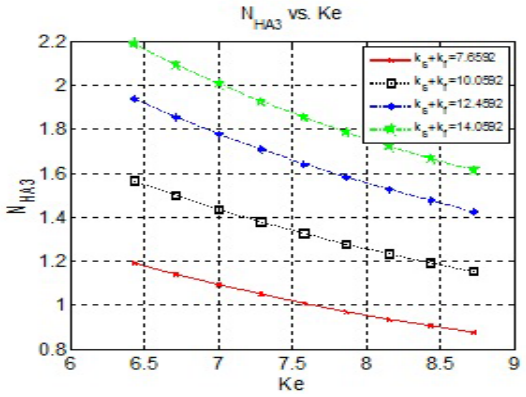

FIG. 2: Variation of the proposed number 3 (N_{HA3}) with effective thermal conductivity (k_e) for different total absolute thermal conductivites of solid and fluid $(k_s + k_f)$

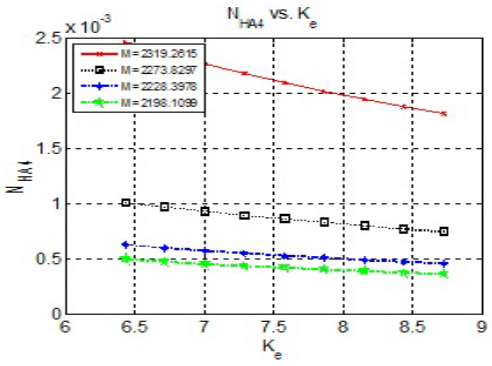

(a)

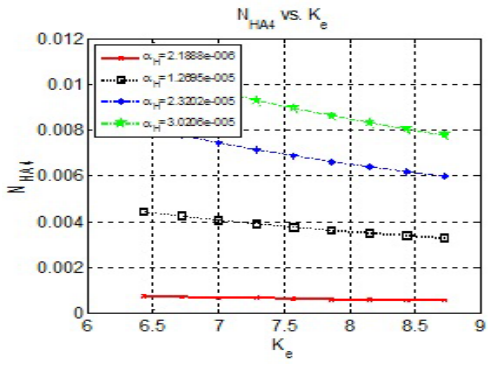

(b)

FIG. 3: Variation of the proposed number 4 (N_{HA4}) with effective thermal conductivity (k_e) for different average system heat capacities (M) at a given $\alpha_H = 2.3202 \times 10^{-5}$ and with different hydraulic diffusivities of the fluid-saturated porous medium α_H at a given M = 2273.83

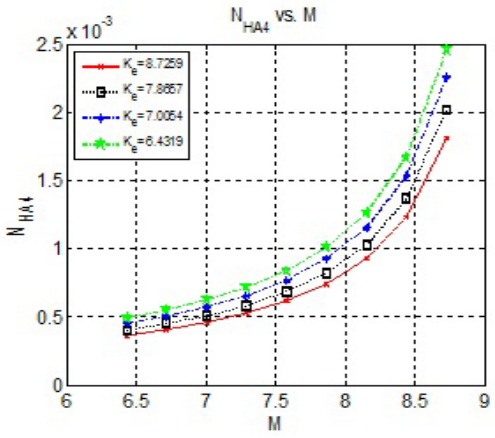

(a)

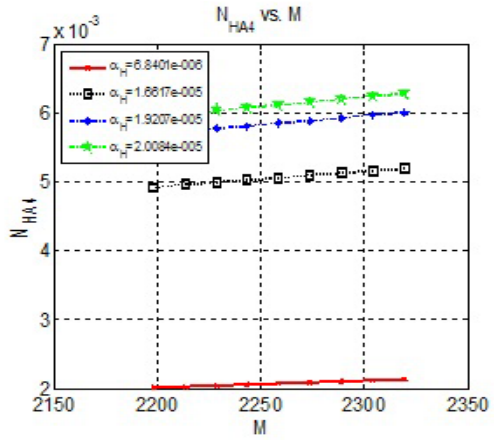

(b)

FIG. 4: Variation of the proposed number 4 (N_{HA4}) with average system heat capacity (M) for different effective thermal conductivities (k_e) at a given $\alpha_H = 5.6184 \times 10^{-4}$ and different hydraulic diffusivities of the fluid-saturated porous medium (α_H) at a given k_e = 7.8657

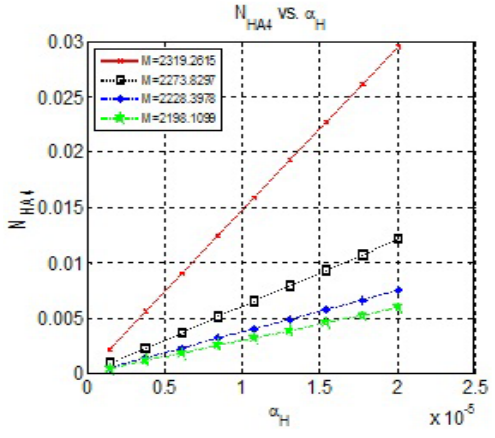

(a)

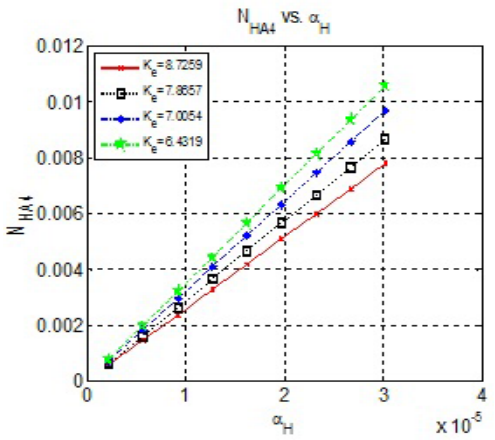

(b)

FIG. 5: Variation of the proposed number 4 (N_{HA4}) with hydraulic diffusivity of the fluid-saturated porous medium (α_H) for different average system heat capacities (M) at a given k_e = 7.8657 and for different effective thermal conductivities (k_e) at a given M = 2273.83

for a particular α_H value, which has a linear step trend [Fig. 5(b)].

Figure 6(a) depicts variation of the proposed number 4 (N_{HA4}) with bulk Prandtl number $((N_{\rm Pr})_b)$ for different the proposed number 5 N_{AH} values, both of the fluid-saturated porous medium as defined by Eq. (10). N_{HA4} increases linearly with increase in $(N_{\rm Pr})_b$ for all N_{AH} values. Since the Prandtl number $N_{\rm Pr}$ is the ratio of convective to conductive heat transfer, increase in N_{HA4} with $(N_{\rm Pr})_b$ implies more heat convection during steam injection. N_{HA4} decreases with increase in N_{AH} for a particular $(N_{\rm Pr})_b$. Figure 6(b) depicts the variation of N_{HA4} with N_{AH} for different $(N_{\rm Pr})_b$ using the same equation. N_{HA4} decreases nonlinearly with increase in N_{AH} for a particular $(N_{\rm Pr})_b$, and N_{HA4} does not show a noticeable change with increase in $(N_{\rm Pr})_b$.

Equation (11) is used to plot Figs. 7(a)–7(d), which depict the variation of the proposed number 4 (N_{HA4}) with the local Nusselt number of the fluid-saturated porous medium (the bulk Nusselt number $(N_{NuL})_b$ for different M, L_c, h_c, and α_H values). N_{HA4} varies linearly with $(N_{NuL})_b$ for various M values [Fig. 7(a)]; however, N_{HA4} is less sensitive to $(N_{NuL})_b$ for low M values than for high M values. The same trend is seen in Figs. 7(b) and 7(c). N_{HA4} versus $(N_{NuL})_b$ shows steep slopes for different h_c values [Fig. 7(d)]. This sharp sloping of the

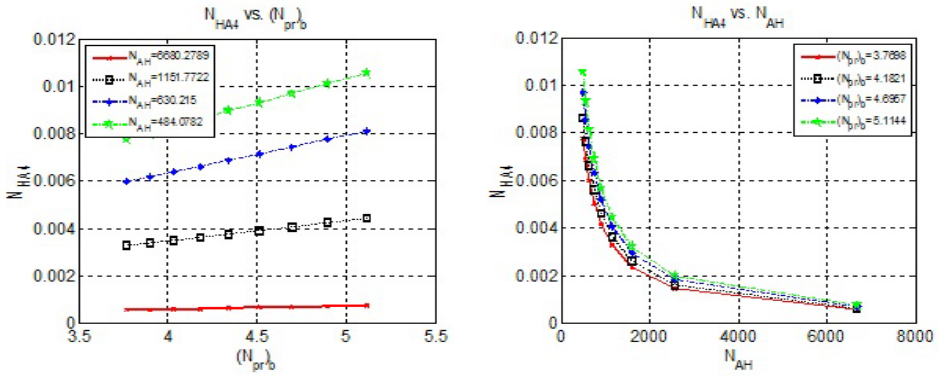

(a) (b)

FIG. 6: Effect of the bulk Prandtl number $(N_{\mathrm{Pr}})_b$ and the proposed number 5 (N_{AH}), both of the fluid-saturated porous medium, on the system's proposed number 4 (N_{HA4})

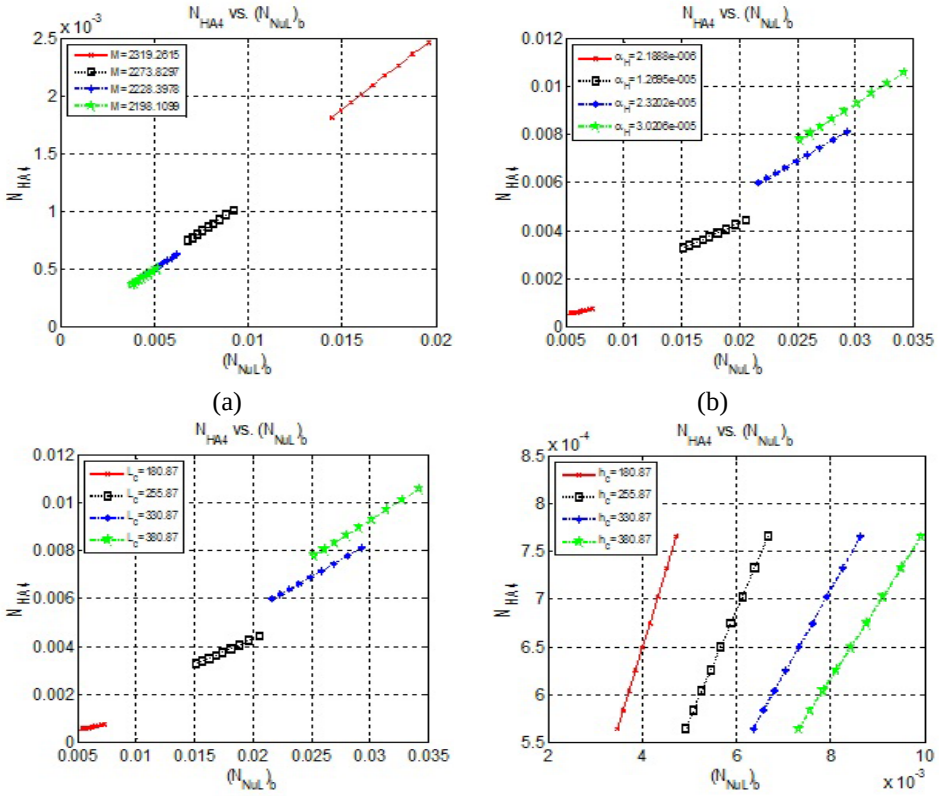

(a) (b)

(c) (d)

FIG. 7: Variation of the proposed number 4 (N_{HA4}) with the local Nusselt number of the fluid-saturated porous medium $((N_{\mathrm{Nu}L})_b)$ for various average system heat capacities (M) at a given $\alpha_H = 2.3202 \times 10^{-5}$, $h_c = 280.87$, $L_c = 255.87$; various hydraulic diffusivity values of the fluid-saturated porous medium (α_H) at a given $M = 2273.83$, $h_c = 280.87$, $L_c = 255.87$; various characteristic lengths (L_c) at a given $\alpha_H = 2.3202 \times 10^{-5}$, $h_c = 280.87$, $L_c = 255.87$; and various convection heat transfer coefficients (h_c) at a given $\alpha_H = 2.3202 \times 10^{-5}$, $M = 2273.83$, $L_c = 255.87$

curve indicates that porous medium's local Nusselt number and N_{HA4} are very sensitive to convective heat transfer coefficient (h_c). Moreover, N_{HA4} increases linearly with increase in $(N_{NuL})_b$ for a particular h_c value. All the previously mentioned figures indicate that more heat conduction takes place when M, a_H, L_c, and h_c are increased, which is related to N_{HA4}. Therefore heat conduction in porous media can be well explained by the proposed number N_{HA4}.

Equation (9) is used to plot Figs. 8(a) and 8(b), which depict the variation of the proposed number 5 (N_{AH}) with fluid density (ρ_f) and fluid viscosity (μ) for different hydraulic diffusivities of the fluid-saturated porous medium (a_H). N_{AH} decreases nonlinearly with increase in ρ_f for a particular α_H value, and N_{AH} decreases with the increase of α_H for the same fluid density [Fig. 8(a)]. Conversely, N_{AH} increases linearly with increase of μ for a particular α_H value, and N_{AH} decreases with the increase of α_H for the same fluid viscosity [Fig. 8(b)]. This indicates that if the fluid momentum diffusivity is increased, N_{AH} increases significantly.

Figures 9(a) and 9(b) show variation of the proposed number 5 (N_{AH}) with fluid kinematic viscosity and hydraulic diffusivities of the fluid-saturated porous medium (α_H) for various α_H and ν values. Figure 9(a) shows that N_{AH} increases linearly with increase in ν for a particular α_H, which reveals the same trend and behavior as commented for Fig. 8(b). This indicates that N_{AH} is sensitive

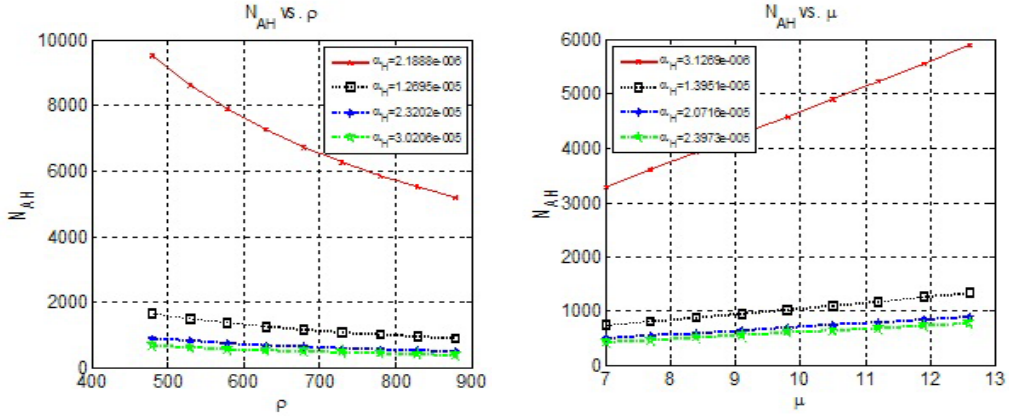

(a) (b)

FIG. 8: Variation of the proposed number 5 (N_{AH}) with fluid density (ρ_f) at a given $\mu = 10$ and fluid viscosity (μ) at a given $\rho_f = 600$ for different hydraulic diffusivities of the fluid-saturated porous medium α_H

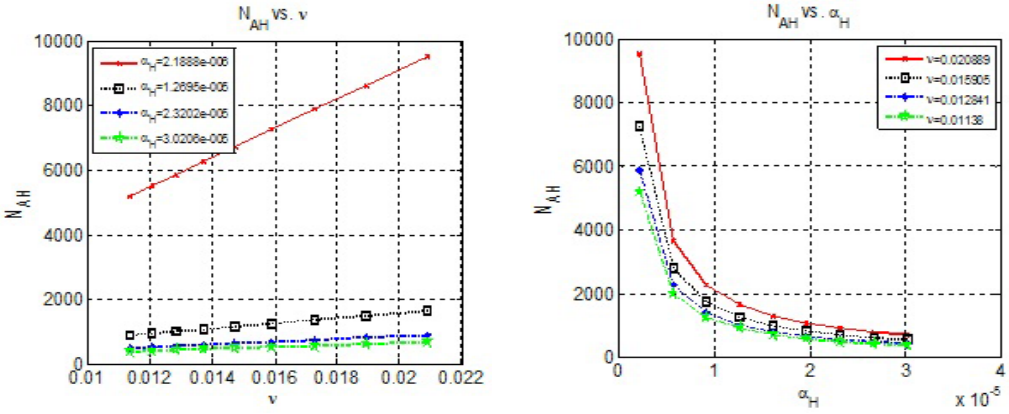

(a) (b)

FIG. 9: Variation of the proposed number 5 (N_{AH}) with fluid kinematic viscosity (ν) and hydraulic diffusivities of the fluid-saturated porous medium α_H for different α_H and ν

to the fluid's momentum diffusivity. N_{AH} decreases nonlinearly with increase in α_H for a particular ν value, and N_{AH} increases with increase in ν for the same system's hydraulic diffusivity [Fig. 9(b)].

The local Peclet number of Eq. (4b) is plotted in Figs. 10(a)–10(c), which depict the variation of N_{PeL} with memory-based fluid velocity (u_m) for various k_e, $\rho_f c_{pf}$, and L_c values. N_{PeL} increases linearly with (u_m) for different (k_e) values [Fig. 10(a)] and decreases with the increase in k_e. For low u_m, k_e has less influence on N_{PeL}. As the degree of memory increases (i.e., increase in u_m), k_e starts to dominate N_{PeL}. The same trend is seen in Fig. 10(b); however, the influence of memory is more pronounced than in the case of k_e. The characteristic length with memory plays a great role on N_{PeL} [Fig. 10(c)], and N_{PeL} increases with increase in L_c and memory becomes more dominant for larger L_c values.

5. CONCLUSIONS

A mathematical model with the inclusion of the memory concept is presented here to introduce new dimensionless numbers during thermal operations in porous media. These numbers can be useful in characterizing reservoir rock and fluid properties. The results and analysis are based on a numerical solution of the model equations using real reservoir data. These results are then employed to explain heat conduction and convection processes in terms of the proposed dimensionless numbers. The case investigated in this study is when the reservoir rock attains the fluid temperature instantaneously. The proposed numbers are well capable of handling the variable rock and fluid properties with time and space and are able to better explain the continuous alteration of rock–fluid behavior. Such information on continuous alteration of rock–fluid rheology is useful for better prediction of reservoir performance. The proposed mathematical tool is used to investigate the effects of temperature on different reservoir parameters, which can also be utilized to investigate the temperature profile by solving the model equations for temperature. The utility of the proposed numbers lies in the ability to characterize the rheological properties of a reservoir if those numbers are known for another analogous reservoir, thus eliminating the need for rigorous investigation.

ACKNOWLEDGMENTS

The authors would like to acknowledge the support provided by the Deanship of Scientific Research (DSR)

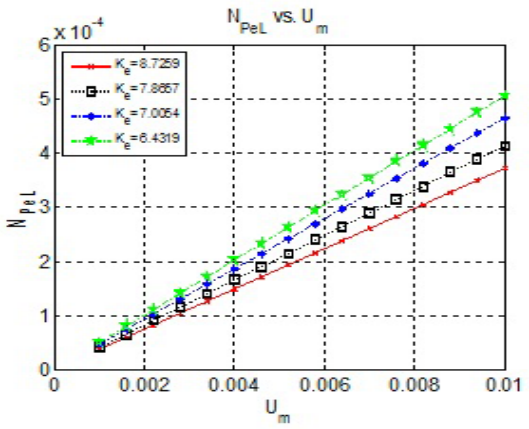

(a)

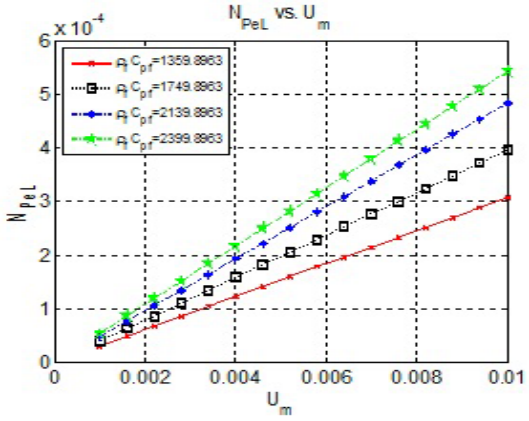

(b)

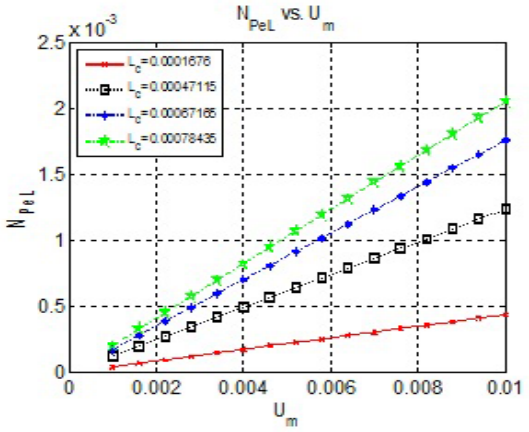

(c)

FIG. 10: Variation of N_{PeL} with (u_m): **(a)** for various (k_e) at a given $\rho_f c_{pf} = 1749.8963$, $L_c = 0.00047115$; **(b)** for various $\rho_f c_{pf}$ at a given $k_e = 7.8657$, $L_c = 0.00047115$; and **(c)** for various (L_c) at a given $\rho_f c_{pf} = 1749.8963$, $k_e = 7.8657$

at King Fahd University of Petroleum and Minerals (KFUPM) for funding this work through project JF100009. Special thanks to associate editor Oronzio Manca of *Journal of Porous Media* for his excellent support in improving the quality of the article. His contribution was in the modifications to the model equations.

REFERENCES

Alazmi, B. and Vafai, K., Analysis of variants within the porous media transport models, *J. Heat Transfer*, vol. **122**, pp. 303–326, 2000.

Caputo, M., Diffusion of fluids in porous media with memory, *Geothermics*, vol. **23**, pp. 113–130, 1999.

Caputo, M., Models of flux in porous media with memory, *Water Resour. Res.*, vol. **36**, no. 3, pp. 693–705, 2000.

Caputo, M. and Plastino, W., Diffusion in porous layers with memory, *Geophys. J. Int*., vol. **158**, no. 1, pp. 385–396, 2004.

Cengel, Y. A. and Ghajar, A. J., *Heat and Mass Transfer: Fundamentals and Applications*, 4th ed., McGraw-Hill, New York, 2011.

Chan, Y. T. and Banerjee, S., Analysis of transient three-dimensional natural convection in porous media, *J. Heat Transfer*, vol. **103**, pp. 242–248, 1981.

Cloot, A. and Botha, J. F., A generalised groundwater flow equation using the concept of non-integer order derivatives, *Water SA*, vol. **32**, no. 1, pp. 1–7, 2006.

Dawkrajai, P., Lake, L. W., Yoshioka, K., Zhu, D., and Hill, A. D., Detection of water or gas entries in horizontal wells from temperature profiles, paper SPE-100050 presented at SPE/DOE Symposium on Improved Oil Recovery, Tulsa, OK, 2006.

De Espiíndola, J. J., Da Silva Neto, J. M., and Lopes, E. M. O., A generalised fractional derivative approach to viscoelastic material properties measurement, *Appl. Math. Comput.*, vol. **164**, no. 2, pp. 493–506, 2005.

Di Giuseppe, E., Moroni, M., and Caputo, M., Flux in porous media with memory: Models and experiments, *Transport Porous Media*, vol. **83**, no. 3, pp. 479–500, 2010.

Hossain, M. E., An experimental and numerical investigation of memory-based complex rheology and rock/fluid interactions, PhD dissertation, Dalhousie University, Halifax, Nova Scotia, Canada, 2008.

Hossain, M. E. and Abu-Khamsin, S. A., Development of dimensionless numbers for heat transfer in porous media using memory concept, *J. Porous Media*, vol. **15**, no. 10, pp. 957–971, 2012.

Hossain, M. E. and Islam, M. R., *An Advanced Analysis Technique for Sustainable Petroleum Operations*, VDM Verlag Dr. Muller Aktiengesellschaft & Co. KG, Saarbr?cken, Germany, p. 655, 2009.

Hossain, M. E., Mousavizadegan, S. H., Ketata, C., and Islam, M. R., A novel memory based stress-strain model for reservoir characterization, *J. Nat. Sci. Sustainable Technol.*, vol. **1**, no. 4, pp. 653–678, 2007.

Hossain, M. E., Mousavizadegan, S. H., and Islam, M. R., The effects of thermal alterations on formation permeability and porosity, *Petrol. Sci. Technol*., vol. **26**, nos. 10–11, pp. 1282–1302, 2008a.

Hossain, M. E., Mousavizadegan, S. H., and Islam, M. R., Rock and fluid temperature changes during thermal operations in EOR processes, *J. Nat. Sci. Sustainable Technol.*, vol. **2**, no. 3, pp. 347–378, 2008b.

Hossain, M. E., Mousavizadegan, S. H., and Islam, M. R., A new porous media diffusivity equation with the inclusion of rock and fluid memories, paper SPE-114287-MS, E-Library, Society of Petroleum Engineers, 2008c.

Hossain, M. E., Mousavizadegan, S. H., and Islam, M. R., Effects of memory on the complex rock- fluid properties of a reservoir stress-strain model, *Petrol. Sci. Technol*., vol. **27**, pp. 1109–1123, 2009a.

Hossain, M. E., Mousavizadegan, S. H., and Islam, M. R., Variation of rock and fluid temperature during thermal operations in porous media, *Petrol. Sci. Technol*., vol. **27**, pp. 597–611, 2009b.

Hossain, M. E., Abu-Khamsin, S. A., and Al-Helali, A., Use of memory concept to investigate temperature profile during a thermal EOR process, paper SPE-SAS-754 presented at the annual Technical Symposium and Exhibition, Al-Khobar, Saudi Arabia, 2011.

Iaffaldano, G., Caputo, M., and Martino, S., Experimental and theoretical memory diffusion of water in sand, *Hydrol. Earth System Sci*., vol. **10**, no. 1, pp. 93–100, 2006.

Kaviany, M., *Principles of Heat Transfer in Porous Media*, 2nd ed., Springer, New York, 1995.

Kaviany, M., *Principles of Heat Transfer*, John Wiley, New York, 2002.

Kolodzie, S., Jr., Analysis of pore throat size and use of the Waxman–Smits equation to determine OOIP in Spindle Field, Colorado, paper SPE-9382 presented at 55th Annual Fall Technical Conference and Exhibition of SPE of AIME, Dallas, Texas, September 21–24, 1980.

Lake, L. W., *Enhanced Oil Recovery*, Prentice Hall, Englewood Cliffs, NJ, 1989.

Lee, D. Y. and Vafai, K., Analytical characterization and conceptual assessment of solid and fluid temperature differentials in porous media, *Int. J. Heat Mass Transfer*, vol. **42**, pp. 423–435, 1999.

Marx, J. W. and Langenheim, R. H., Reservoir heating by hot fluid injection, *Trans. AIME*, vol. **216**, pp. 312–314, 1959.

Nield, D. A. and Bejan, A., *Convection in Porous Media*, 3rd ed., Springer, New York, 2006.

Pittman, E. D., Relationship of porosity and permeability to various parameters derived from mercury injection-capillary pressure curve for sandstone, *AAPG Bull.*, vol. **76**, pp. 191–198, 1992.

Rezaee, M. R., Jafari, A., and Kazemzadeh, E., Relationships between permeability, porosity and pore throat size in carbonate rocks using regression analysis and neural networks, *J. Geophys. Eng*., vol. **3**, pp. 370–376, 2006.

Satman, A., Zolotukhin, A. B., and Soliman, M. Y., Application of the time-dependent overall heat-transfer coefficient concept to heat-transfer problems in porous media, *Soc. Petrol. Eng. J*., February, pp. 107–112, 1984.

Spillette, A. G., Heat transfer during hot fluid injection into an oil reservoir, *J. Can. Petrol. Technol*., Oct.-Dec., pp. 213–218, 1965.

Vafai, K., *Handbook of Porous Media*, Marcel Dekker, New York, 2000.

van Poollen, H. K., et al., *Fundamentals of Enhanced Oil Recovery*, PennWell, Tulsa, OK, 1980.

Wang, Z. and Horne, R. N., Analyzing wellbore temperature distributions using nonisothermal multiphase flow simulation, paper SPE-144577 presented at the SPE Western North American Regional Meeting, Anchorage, AK, 2011.

Weibo, S., Ehlig-Economides, C., Zhu, D., and Hill, A. D., Determining multilayer formation properties from transient temperature and pressure measurements in commingled gas wells, paper SPE-131150 presented at the CPS/SPE International Oil and Gas Conference and Exhibition, Beijing, China, 2010.

Willman, B. T., Valleroy, V. V., Runberg, G. W., Cornelius, A. J., and Powers, L. W., Laboratory studies of oil recovery by steam injection, *J. Pet. Techn. Trans. AIME*, vol. **222**, pp. 681–690, 1961.

Yoshioka, K., Zhu, D., Hill, A. D., and Lake, L. W., Interpretation of temperature and pressure profiles measured in multilateral wells equipped with intelligent completions, paper SPE-94097 presented at SPE Europec/EAGE annual conference, Madrid, Spain, 2005a.

Yoshioka, K., Zhu, D., Hill, A. D., Dawkrajai, P., and Lake, L. W., A comprehensive model of temperature behavior in a horizontal well, paper SPE-95656 presented at SPE Annual Technical Conference and Exhibition, Dallas, TX, 2005b.

Yoshioka, K., Zhu, D., Hill, A. D., Dawkrajai, P., and Lake, L. W., Detection of water or gas entries in horizontal wells from temperature profiles, paper SPE-100209 presented at SPE Europe/EAGE Annual Conference and Exhibition, Vienna, Austria, 2006.

Yoshioka, K., Zhu, D., Hill, A. D., Dawkrajai, P., and Lake, L. W., Prediction of temperature changes caused by water or gas entry into a horizontal well, paper SPE-100209 presented at SPE Production and Operations, November, pp. 425–433, 2007.

Yoshioka, K., Zhu, D., Hill, A. D., and Lake, L. W., A new inversion method to interpret flow profiles from distributed temperature and pressure measurements in horizontal wells, paper SPE-109749 presented at SPE Production and Operations, November, pp. 510–521, 2009.

Zavala-Sanchez, V., Dentz, M., and Sanchez-Vila, X., Characterization of mixing and spreading in a bounded stratified medium, *Adv. Water Resour.*, vol. **32**, no. 5, pp. 635–648, 2009.

APPENDIX

To determine the temperature distribution with space and time, the energy balance equation is considered as the governing equation separately for both rock and fluid. The partial differential equations have a familiar form because the system has been averaged over representative elementary volumes (REV). A right-handed Cartesian coordinate system is considered where the x axis is along the reservoir length. The conventional forms of energy balance equations are available in literature (Spillette, 1965; van Poollen et al., 1980; Chan and Banerjee, 1981; Lake, 1989; Satman et al., 1984; Kaviany, 2002; Dawkrajai et al., 2006; Yoshioka et al., 2006, 2007, 2009; Hossain et al., 2008a, 2008b, 2009b; Weibo et al., 2010; Cengel and Ghajar, 2011; Wang and Horne, 2011). However, if we neglect the kinetic energy, the viscous dissipative heating, the thermal energy change caused by fluid expansion, the potential energy, and the gravity work, the general form of the differential energy balance equations in three dimensions may be given as (Kaviany, 1995; Lee and Vafai, 1999; Alazmi and Vafai, 2000; Nield and Bejan, 2006)

$$\nabla.\left[\left(1-\phi\right)k_s\nabla T_s\right]=\left(1-\phi\right)\rho_s c_{ps}\frac{\partial T_s}{\partial t}+\frac{h_c}{L}\left(T_s-T_f\right) \tag{A1}$$

$$\nabla.\left(\phi k_f\nabla T_f\right)-\rho_f c_{pf}\left(\overline{u}_m.\nabla T_f\right)=\phi\rho_f c_{pf}\frac{\partial T_f}{\partial t}+\frac{h_c}{L}\left(T_f-T_s\right) \tag{A2}$$

where

$$\rho_f c_{pf}=\rho_w c_{pw}S_w+\rho_o c_{po}S_o+\rho_g c_{pg}S_g \tag{A3}$$

$$\rho_f=\rho_w S_w+\rho_o S_o+\rho_g S_g \tag{A4}$$

$$S_w + S_o + S_g = 1 \tag{A5}$$

In Eqs. (A1) and (A2), T_s and T_f are the rock matrix and fluid temperatures, respectively. These represent the thermal state of each phase in the same REV.

Taking into account a porous medium of uniform cross-sectional area and homogeneous along the x axis, and considering that the thermal conductivities of the fluid and solid rock matrix are temperature independent and are constant along the medium, Eqs. (A1) and (A2) can be written in one-dimensional form as

$$(1-\phi)\,k_s\frac{\partial^2 T_s}{\partial x^2} = (1-\phi)\,\rho_s c_{ps}\frac{\partial T_s}{\partial t} + \frac{h_c}{L}(T_s - T_f) \tag{A6}$$

$$\phi k_f\frac{\partial^2 T_f}{\partial x^2} - \rho_f c_{pf} u_m\frac{\partial T_f}{\partial x} = \phi\rho_f c_{pf}\frac{\partial T_f}{\partial t} + \frac{h_c}{L}(T_f - T_s) \tag{A7}$$

where

$$k_f = k_w S_w + k_o S_o + k_g S_g \tag{A8}$$

Equation (A6) can be rearranged after setting $k_{s_{\text{eff}}} = (1-\phi)\,k_s$ as

$$\frac{h_c}{L}(T_f - T_s) = (1-\phi)\,\rho_s c_{ps}\frac{\partial T_s}{\partial t} - k_{s_{\text{eff}}}\frac{\partial^2 T_s}{\partial x^2} \tag{A9}$$

Substituting Eq. (A9) into Eq. (A7) after setting $k_{f_{\text{eff}}} = \phi k_f$ in Eq. (A7) yields

$$k_{f_{\text{eff}}}\frac{\partial^2 T_f}{\partial x^2} - \rho_f c_{pf} u_m\frac{\partial T_f}{\partial x} = \phi\rho_f c_{pf}\frac{\partial T_f}{\partial t} + (1-\phi)\,\rho_s c_{ps}\frac{\partial T_s}{\partial t} - k_{s_{\text{eff}}}\frac{\partial^2 T_s}{\partial x^2} \tag{A10}$$

If the temperatures of the fluid and solid rock are the same, the preceding energy balance equation, Eq. (A10), can be written as

$$(k_{s_{\text{eff}}} + k_{f_{\text{eff}}})\frac{\partial^2 T}{\partial x^2} - \rho_f c_{pf} u_m\frac{\partial T}{\partial x} = \{(1-\phi)\,\rho_s c_{ps} + \phi\rho_f c_{pf}\}\frac{\partial T}{\partial t} \tag{A11}$$

Defining the average system heat capacity as

$$M = (1-\phi)\,\rho_s c_{ps} + \phi\rho_w c_{pw} S_w + \phi\rho_o c_{po} S_o + \phi\rho_g c_{pg} S_g \tag{A12}$$

and substituting Eq. (A3) into Eq. (A12) yields

$$M = (1-\phi)\,\rho_s c_{ps} + \phi\rho_f c_{pf} \tag{A13}$$

Substituting Eq. (A13) into Eq. (A11) yields

$$M\frac{\partial T}{\partial t} + \rho_f c_{pf} u_m\frac{\partial T}{\partial x} - k_e\frac{\partial^2 T}{\partial x^2} = 0 \tag{A14}$$

Where,

$$k_e = k_{s_{\text{eff}}} + k_{f_{\text{eff}}} \tag{A15}$$

The first term of Eq. (A14) is the accumulation of energy, the second term is the thermal energy transported by convection, and the third term is thermal energy transported by heat conduction.

Equation (A14) can be transformed into dimensionless form using the defined non-dimensional parameters as described in Section 2. Substituting the above transformations in to Eq. (A14) yields:

$$M\frac{T_i k}{\phi\mu c_t \mathrm{L}^2}\frac{\partial T^*}{\partial t^*} + \rho_f c_{pf} u_m\frac{T_i}{L}\frac{\partial T^*}{\partial x^*} - k_e\frac{T_i}{\mathrm{L}^2}\frac{\partial^2 T^*}{\partial x^{*^2}} = 0 \tag{A16}$$

$$M\frac{k}{\phi\mu c_t}\frac{\partial T^*}{\partial t^*} + \frac{L_c\rho_f c_{pf} u_m}{k_e}k_e\frac{L}{L_c}\frac{\partial T^*}{\partial x^*} - k_e\frac{\partial^2 T^*}{\partial x^{*^2}} = 0 \tag{A17}$$

Finally Eq. (A17) can be written in terms of $N_{\mathrm{Pe}L}$ and N_{HA4} as:

$$N_{HA4}\frac{\partial T^*}{\partial t^*} + N_{\mathrm{Pe}L}\frac{L}{L_c}\frac{\partial T^*}{\partial x^*} - \frac{\partial^2 T^*}{\partial x^{*^2}} = 0 \tag{A18}$$

where,

$$N_{HA4} = \frac{M\alpha_H}{k_e}$$